Summer Student Program
at the Joint Institute for Nuclear Research

Frank Laboratory of Neutron Physics
Department of Raman Spectroscopy
(Centre «Nanobiophotonics»)

Research of plasmonic nanostructures within the pores of silicon oxide for enhanced Raman spectroscopy

Dzmitry Yakimchuk
Scientific and Practical Materials Research Centre of NAS of Belarus

Supervisor:
Dr Grigory Arzumanyan
Head, Department of Raman Spectroscopy
(Centre «Nanobiophotonics»)

Dubna, 2015

Introduction

Optical microscopy is one of the major methods of research of properties, quality control and diagnostics of liquid and solid media in materials physics, industrial production, chemistry, biology and medicine [1]. Modern fluorescent, confocal and laser scanning microscopes are widely used to obtain spatial, including 3D, images of materials' and objects' structure in various domains of natural sciences, industry and medicine. Optical microscopy grows in its importance with the development of modern nanotechnology, biotechnology, methods of diagnostics and treatment of most dangerous for mankind diseases [2].

The traditional methods of optical microscopy that operate in fluorescent, reflecting and transmitting modes have been successfully complemented with new high resolution techniques of the confocal fluorescent and Raman microscopy since the time when coherent laser sources of radiation and new high-efficient fluorescent tags (organic dyes, semiconductor nanostructures, quantum dots) were applied. The confocal laser fluorescence microscopy with extrinsic agents that label the sample is widely applied at present and has serious advantages, in comparison to the traditional microscopy of transmitted and reflected light. It is related to high intensity of the fluorescent signal, high space resolution, possibility to apply several fluorophores connected selectively to different structural components of the cell, etc. At the same time, florescent labels often leads to photobleaching of biosamples, thus limiting their sensitivity.

Short theoretical background

Along with the traditional fluorescence or Raman microscopy, nonlinear optical microscopy has been developing intensively [3]. With this method, the generated signal that forms the contrast mechanism of the image depends non-linearly on the excitation intensity. The non-linear optical microscopy includes Two-Photon (Multi-Photon) Fluorescence microscopy (TPEF), the microscopy based on the Generation of the Second (Third) Harmonic (SGH, THG), the sum or differential frequencies (SFG, DFG), as well as the four-wave-mixing microscopy including the vibrational coherent anti-Stokes Raman scattering (CARS) [4]. As all the above mentioned types of non-linear microscopy are based on various non-linear phenomena, they may bear different on principle information about the object under study and successfully complement each other. High-intensity pico- or femto- second lasers are used to initiate several non-linear optical phenomena and for simultaneous generation of several images [5]. In particular, CARS is a third-order nonlinear optical process involving in interactions between a pump beam of frequency ω_p, a Stokes beam of frequency ω_s, and a CARS signal at the anti-Stokes frequency of $\omega_{as}=2\omega_p-\omega_s$ generated in the phase matching direction (see the Fig. 1). The sample is stimulated through a four-wave mixing process. The vibrational contrast in CARS is created when the frequency difference $\Delta\omega= \omega_p-\omega_s$ between the pump and the Stokes beams is tuned to be resonant with a Raman-

active molecular vibration. In this case the resonant oscillators are coherently driven by the excitation fields, thereby generating a strong and directed anti-Stokes signal in comparison to spontaneous Raman microscopy.

Along with the CARS signal, usually, the sample (non-linear medium) will generate the second harmonic signal at the frequencies $2\nu_s$ and $2\nu_p$ or their combination $\nu_s \pm \nu_p$; besides, if the medium is tagged with two-photon active chromoforms, two-photon fluorescence signals will be emitted as well. All the signals enumerated in the example may have comparable intensity sufficient for detection and well spread in the spectrum. In case of many registration channels, images completely different in their physical nature can be formed in the microscope thus reciprocally enriching data on the object. This type of microscopy can be called the multi-channel non-linear optical microscopy. Comparing CARS with traditional Raman spectroscopy is given that the first one will show intensity signal gain till the 4 order.

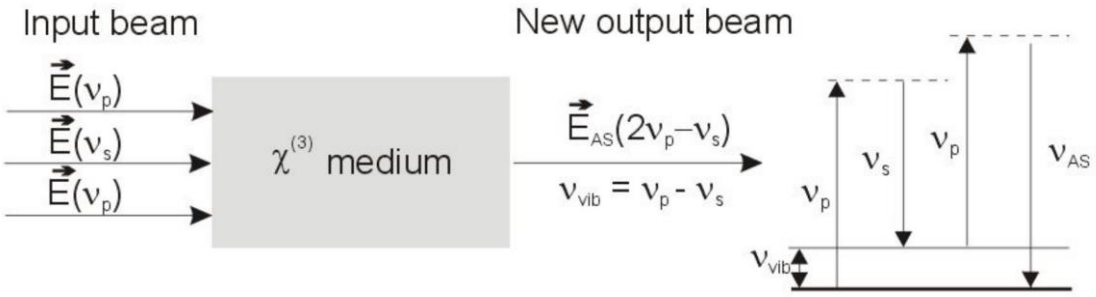

Fig.1. Diagram of the coherent anti-Stokes Raman scattering process.
ν_p – pumping wave $E(\nu_p)$, ν_s – Stokes component of the Raman scattering $E(\nu_s)$, vibrational resonance ν_{vib}, ν_{as} – anti-Stokes component of the Raman scattering $E(\nu_{as})$ on the vibrational resonance ν_{vib}

Another technique, which allows to achieve enhancement of the Raman signal (10^4–10^6 times), is known as Surface Enhanced Raman Spectroscopy (SERS). SERS is a technique that was developed to detect extremely small quantities of molecules by determining their characteristic Raman signal [6, 7]. The high sensitivity of SERS is mainly due to electromagnetic interaction given by an effective, evanescent field enhancement on the metal surface based on the excitation of surface plasmon-polariton modes. By generating metallic nanostructures with different shapes/dimensions, it is possible to tune the plasmon resonance. Moreover, 3D metallic nanostructures with particularly large active surfaces lead to the increase of the sensitivity since more molecules are adsorbed in the focus area of the laser in comparison to conventional 2D SERS active surfaces.

The intrinsic properties of the metal nanostructures can be tuned by controlling their shape, size, and crystallinity. To date, many approaches have been developed to prepare Ag nanostructures in different shapes, like wires, prisms, cubes and others. Recently, extensive interest has been expressed in the synthesis of more complex hierarchical structures that are ideally composed of nanocrystals

(particles, rods, ribbons, and so forth) arranged in a particular way as well as their growth mechanism. These types of materials not only possess improved properties originating from their building blocks but also solve the problem of nanomaterial agglomeration. Additionally, they find applications in many fields, especially in (bio)-sensoric technology based on Raman spectroscopy.

In this work we have used plasmonic silver nanostructures which were formed by template synthesis. Self-organized silver nanostructures where grown in porous Si/SiO_2 matrix fabricated by ion track technology [8]. The different silver nanostructures with shapes like “sunflowers”, “azalea”, “corn” and others (Fig. 2) were realized by applying wet-chemical electroless deposition. These plasmonic structures with large surface areas, composed of major trunks and many hierarchical side branches, provide a great opportunity to improve their properties for SERS application.

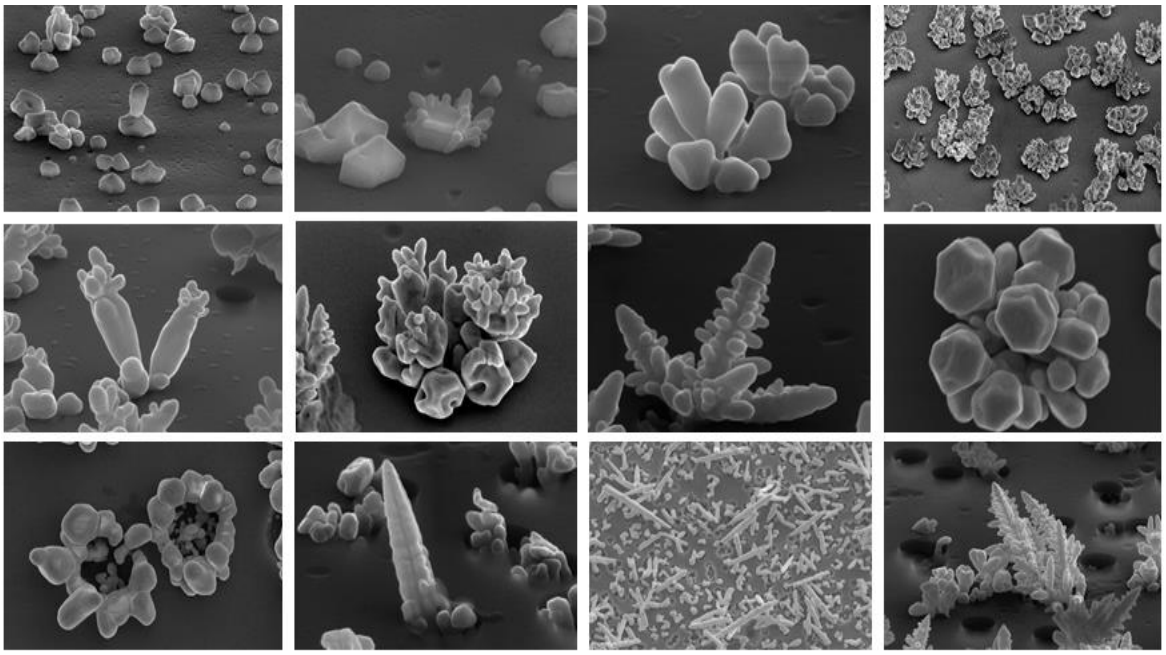

Fig.2. Different shapes of silver plasmonic nanostructures that were formed by ion track technology (scale 1×1 μm)

Experimental set-up: CARS microscope at JINR

In 2011 the CARS microscope (Fig. 3) manufactured at the “SOLAR TII” company in Minsk, Belarus was supplied to JINR, Dubna.

In the given CARS microscope a diod-pump $Nd:YVO_4$ picosecond laser is used as a source of the Stokes wave; it has the wave length of 1064 nm, pulse duration of 7 ps and output power of 5W at the pulse repetition rate of 85 MHz. Only a small portion of radiation was directed to the microscope, the main part of radiation was used for the second harmonic intracavity generation to be applied for the synchronous pumping of the optical parametric oscillator (SOPO). That provided generation of picosecond pulses tunable from 690 nm to 990 nm, with pulse duration of 6 ps and output power up to 0.3W at the repetition rate of 85

MHz. The radiation of two lasers was combined in space with the system of dichroic mirrors and through a computer-controlled galvano-scanner directed to the inverted microscope assembled on the NIKON 2000S mount, with the wide aperture (60x *NA*-1.2) water-immersion lense Olimpus UPLSAPO 60XW installed on the Z piezo-scanner with the minimal step of 100 nm and the scanning range of 80 microns.

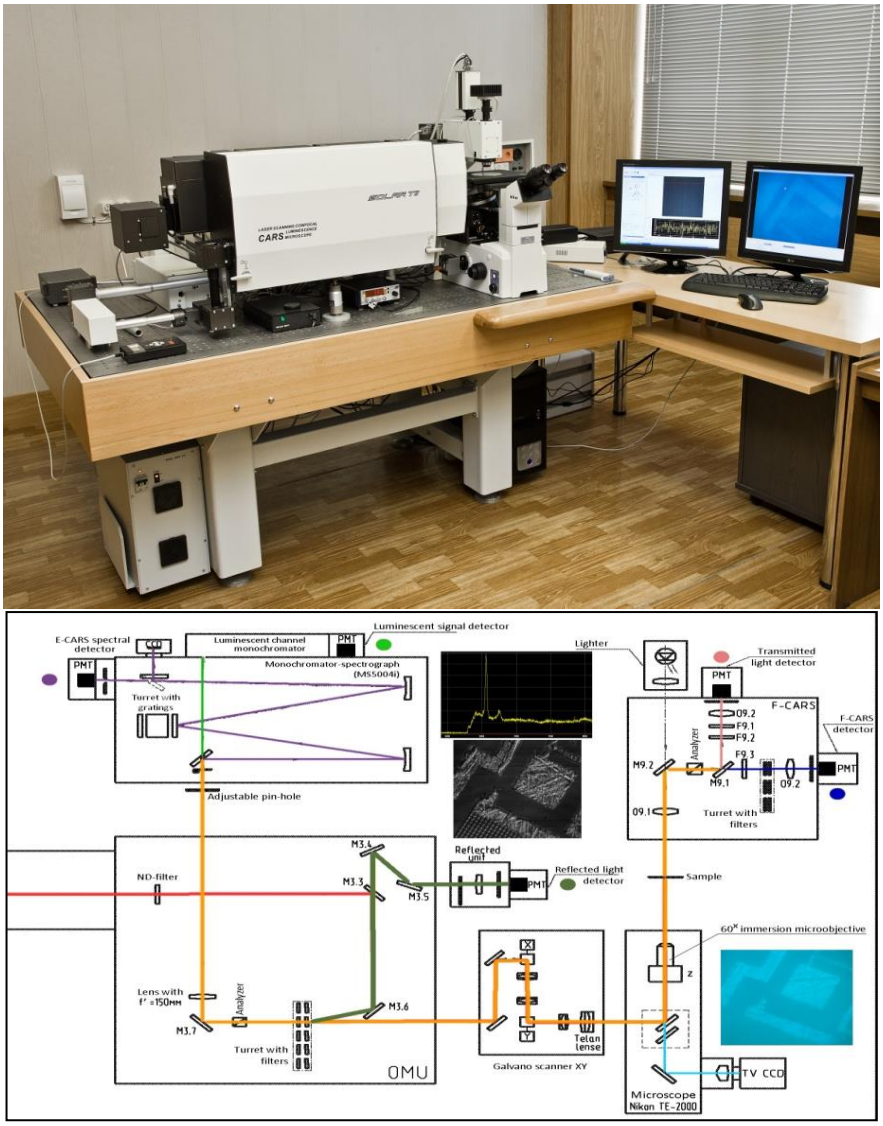

Fig.3. The general view (upper picture) and the optical layout of the CARS microscope with the 6 registration channels installed at JINR, Dubna in 2011

The microscope is also equipped with a system of collimators, dichroic mirrors and filters whose installment and change is done automatically on PC commands. The signals generated on the sample both parallel to pumping (F-CARS) and backward (E-CARS) are collected with the corresponding collimators, optically filtered of the initiating beams and are directed to the corresponding registration channels for further digital processing and image construction. As the sample is illuminated with high-intensity laser beams, at certain conditions the sample can generate, in addition to the anti-Stokes Raman signal, also signals of two-photon fluorescence (TPE), the second harmonic (SHG), and other non-linear

optical signals that occur in the sample. For this purpose, the microscope is equipped with 6 independent registration channels, two in the forward direction and four in the backward direction. Four out of possible six channels can simultaneously detect and process the image. Sorting signals of various origins into channels is conducted automatically by the controlled system of spectro-splitters and notch-filters, dichroic mirrors and switchable interference filters. The input ports of excitation lasers are equipped with computer-controlled shutters to open the laser radiation input port only at the time of the sample scanning and prevent the action of the fixed-in-space focused beams on the sample. The microscope is also equipped with polarization devices to control polarization of the excitation radiation and registration channels polarization that allows one to organize polarization detection of signals, including the so-called P-CARS signal. The system of the sample scanning and the following digital processing of images provide selective choice of the scanning zone and the installment of various resolution of the image from 100x100 pixels to 1000x1000 pixels.

The CARS microscope software provides operational control of the main system parameters, such as spectral splitting of the signal and its space distribution along the registration channels, the scanning region, space resolution, enlarging the image (Zoom) with selection of the scanning zone, accumulation of the signal according to the scan series, simultaneous visualization of up to 4 images that correspond to different registration channels on the computer monitor screen, construction of 3D images with registration of still-frame images at automatic stepwise shift of the scanning plane with the controlled scanning step and the following emulating of 3D images on the computer monitor screen, recording of the images in the electronic form and their reproduction for mathematical processing.

As distinguished from the one-photon fluorescent imaging, the CARS microscopy uses laser sources with wavelengths in the infrared region of the spectrum, far from the biological molecules absorption bands; besides, the picoseconds pulses does not lead to considerable heat load because of the short action in a definite scanning zone of the bio-object; non-linear interactions with molecules are far from the ionization thresholds. The value of the radiation load on the sample is determined by several factors, such as the mean power of the pump lasers, duration of the action on the so-called single pixel of the image (the sample region), the scanning rate, the scanning region (area), the image resolution. In real conditions of the cell image registration, with the shutter open only during scanning and the mean power of the laser radiation up to 100 mW, the scanning zone not less than 20x20 micron, the scanning rate ~ 500 ms, and resolution of 500 x 500 pixels, we have not detected any signals of photo degradation of the cell at continuous scanning up to 500 stills. In 2015 microscope was upgraded: a green diode laser (532 nm, 18 mW) and «100x» objective lens with high numerical aperture (0.95) were complemented to the “CARS” microscope.

Experimental part

Experiments were carried out with some biological samples and organic dyes. Membrane proteins are among the most important biological targets: they comprise about one-third of the human genome [9], perform the main functions of biological membranes, and are of great interest to the pharmaceutical industry, around 60 % of all current drugs targeting membrane proteins [10]. Bacteriorhodopsin (BR) is one of the best characterized membrane proteins, which has been studied by a vast array of biophysical techniques [11], including Raman spectroscopy. All of the above makes it interesting for CARS experiments. In Fig. 4 and Fig. 5 are shown the advantages of using this method in the study of BR crystals.

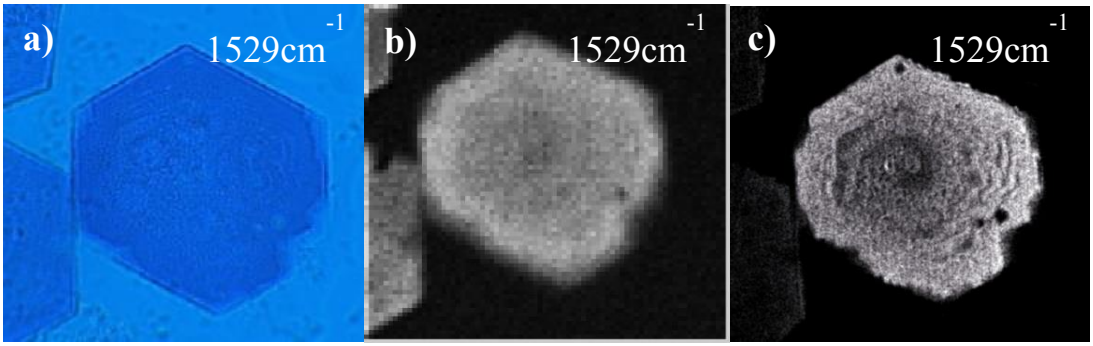

Fig.4. Comparison of images of the crystal: a) photomicrograph of BR crystal from camera; b) Raman image of the same BR crystal with high-aperture objective, *NA* = 1.2, scan area 48×48 μm, scan time ~ one hour, resolution - 100×100 points; c) CARS image of BR crystal with high-aperture objective, *NA* = 1.2, scan area 48×48 μm, scan time ~ few seconds, resolution 250×250 points

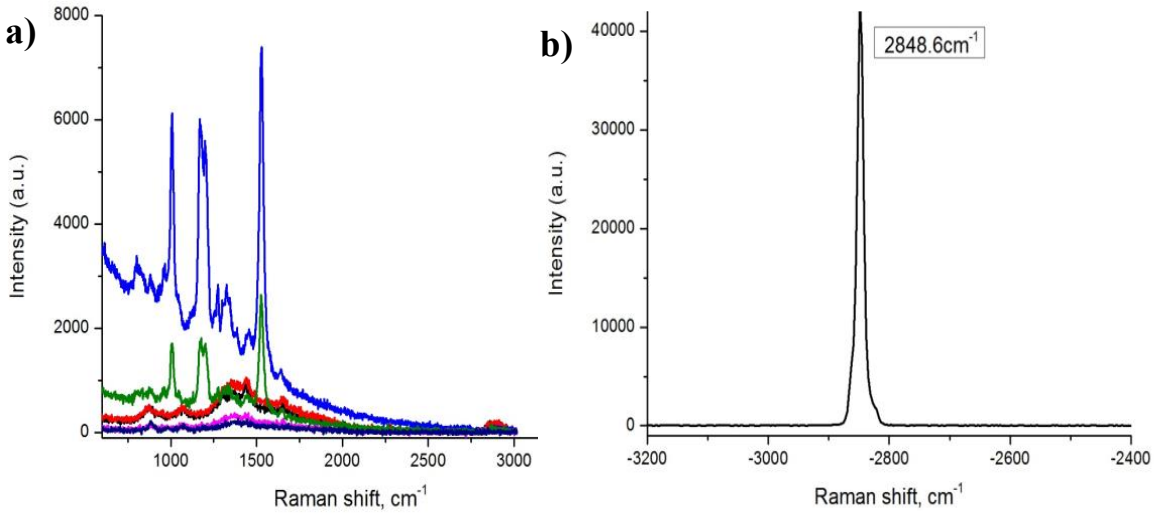

Fig.5. Comparison of typical Raman spectra (a) of BR and CARS (b) of BR

The main focus in the present research was on the development of SERS method. The standard dye molecule like Rhodamine 6G (R6G) was used to study

the SERS induced by silver plasmonic nanostructures in “sunflower” shape. The concentration of the dye was 10^{-6} M. Experiments were carried out by two lasers with wavelengths 532 nm (green) and 633 nm (red). The laser power at the samples' surface was kept at 150 μW, 100 μW, 50 μW, 5μW and 2.5 μW. The scan time was 0.5 s. The laser beam was focused through a «100×» microscope objective lens with *NA* = 0.95. The resulting spot diameter was about 340 nm for green laser and about 400 nm for red one. These dimensions match the size of silver conglomerates that amplifies the Raman signal.

It is well known that in the green region of the spectrum R6G exhibits strong fluorescent properties [12]. This strongly limits the availability to register spontaneous Raman signal from R6G by the green laser to compare it with the SERS signal. However, the characteristic Raman peaks of the analyte (601 cm^{-1}, 759 cm^{-1}, 1171 cm^{-1}, 1280 $cm^{-}1$, 1350 cm^{-1}, 1498 cm^{-1}, 1565 cm^{-1} and 1639 cm^{-1}) are clearly detected in the SERS spectrum (Fig. 6). Some shifting of the peaks is caused by the features of SERS effect.

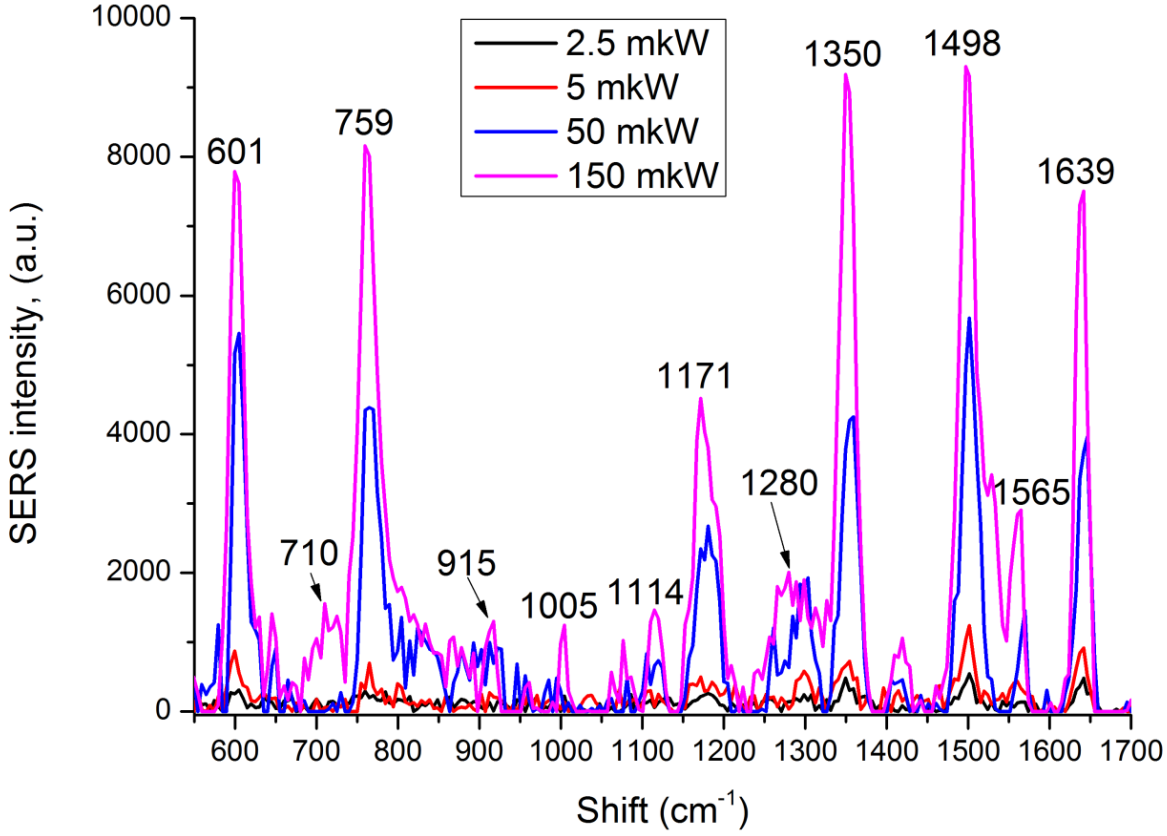

Fig.6. SERS spectrum of R6G 10^{-6} M excited by the green laser with various powers: 150 μW, 100 μW, 50 μW, 5μW and 2.5 μW

Implementing the SERS measurements with the red laser (633nm) we succeeded in the estimation of the SERS enhancement factor (*EF*). Firstly, we measured the conventional Raman signal from R6G with at the concentration of 10^{-2} M and laser power of 4 mW (Fig. 6). And then we realized our SERS experiment with much lower concentration and lower laser powers. The best result was obtained at 5 μW (Fig. 7): $EF \sim 10^{7}$.

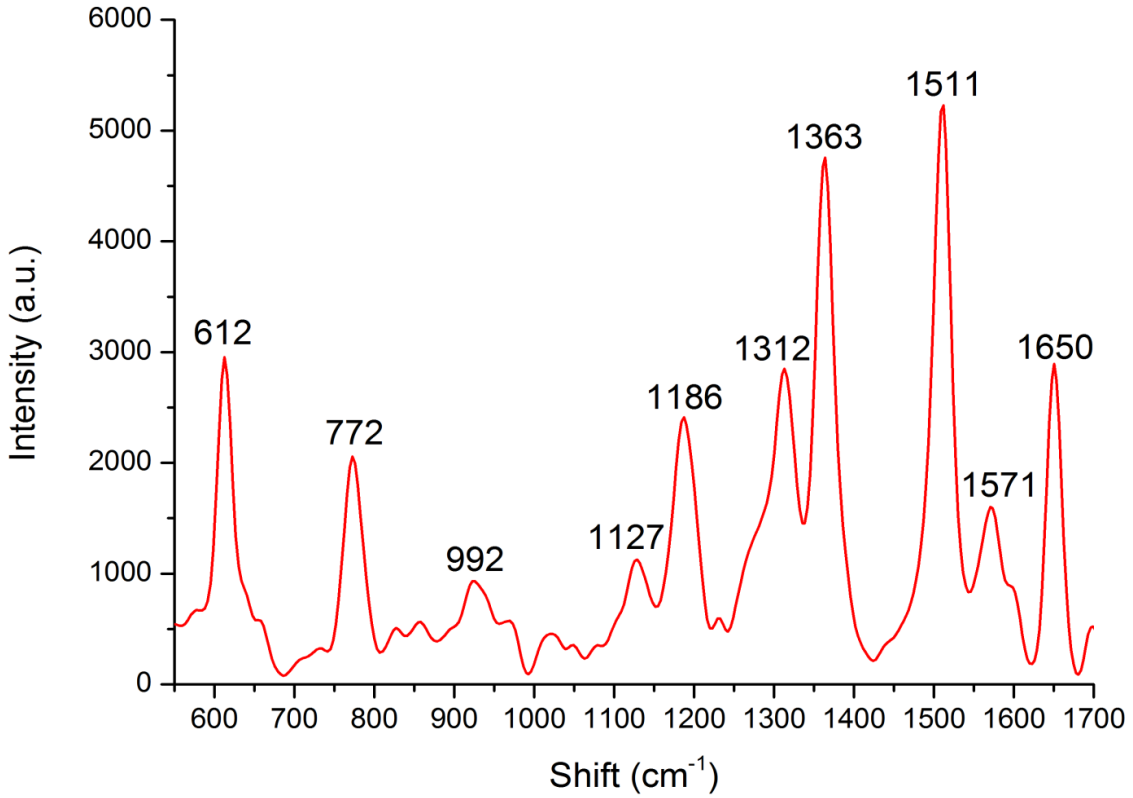

Fig.6. Raman spectra of R6G (10^{-2} M) excited by the red laser, 4 mW

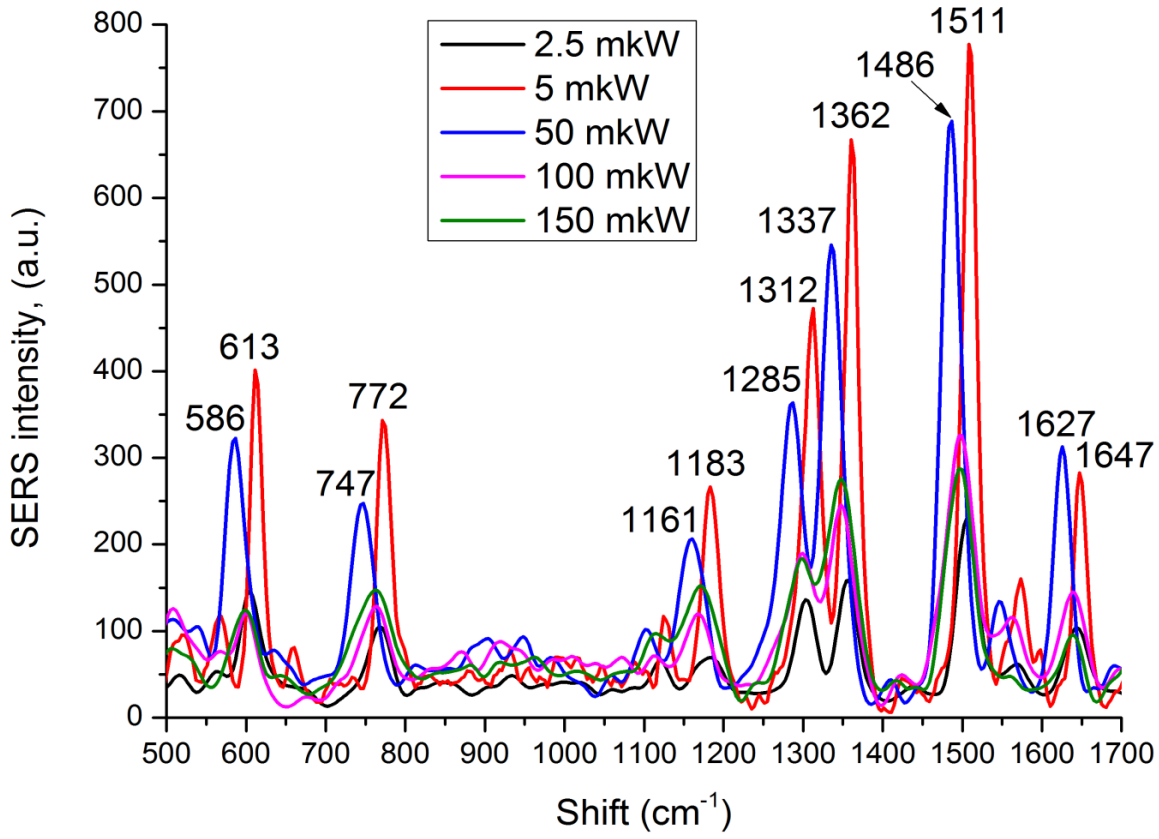

Fig.7. SERS spectra of R6G 10^{-6} M excited by the red laser at powers: 150 μW, 100 μW, 50 μW, 5μW and 2.5 μW

Conclusions

In this work it has been shown two methods (CARS and SERS) to enhance the Raman signal. We performed CARS experiments with BR crystals to show the advantages of CARS method in comparison with conventional Raman scattering. For studying SERS technique we have used special plasmonic substrates with silver nanostructures, which were formed by ion track technology. The silver nanostructures with "sunflower" shape show high SERS sensitivity allowing the detection of R6G dye molecules with low concentration. This indicates that silver nanostructures grown in etched ion tracks are an active substrate for enhancement of Raman signal. Such nanostructures can be used as biosensors operating on the Raman signal amplification effect.

Acknowledgments

I would like to thank Prof. S.Z. Pakuliak, the Director of the JINR University Centre, the management of the UC and the organizers (Elena Karpova and Julia Rybachuk) for their support and opportunity to participate in this 2015 Summer Student Program. I am very grateful to my supervisor Dr Grigory Arzumanyan for the general coordination of my research activities and very good working conditions during the whole period of Summer School. I would like to thanks the staff members of the Raman Spectroscopy department Nelly Doroshkevich and Kahramon Mamatkulov for their valuable assistance in the experiments. I am also greatly thankful to my Belarusian supervisor Dr Egor Kaniukov for his help with synthesizing the plasmonic SERS substrates used in the present work.

References

[1] E.M. Ślater, H.S. Ślater, "Light and electron microscopy", Cambridge, 1993, University Press.

[2] Robert H Webb, "Confocol optical microscopy Rep. Progress", Phys. **59**, (1996), 427–471.

[3] M.D. Duncan, J. Reintjes, and T.J Manuccia, "Scanning coherent anti-Stokes Raman microscope", Opt. Lett. **7**, 350–352 (1982).

[4] A. Volkmer, "Vibrational imaging and microspectroscopies based on coherent anti-Stokes Raman scattering microscopy", J. Phys. D: Appl. Phys. **38**, R59–R81 (2005).

[5] J.-X. Cheng and S. Xie, "Coherent Anti-Stokes Raman Scattering Microscopy: Instrumentation, Theory, and Applications", J. Phys. Chem. B **108**, 827–840 (2004).

[6] Jiang et al., "Single-molecule Raman spectroscopy at the junctions of large Ag nanocrystals", J. Phys. Chem. B **107**, 9964–9972 (2003).

[7] M. Futamata, “Single molecule sensitivity in SERS: importance of junction of adjacent Ag nanoparticles”, Faraday Discuss **132**, 45-61 (2006).
[8] V. Sivakov, “Silver nanostructures formation in porous Si/SiO_2 matrix”, J. of Crystal Growth **400**, 21-26 (2014).
[9] A. Krogh, B. Larsson, G. von Heijne, EL. Sonnhammer, “Predicting transmembrane protein topology with a hidden Markov model: application to complete genomes”, J Mol Biol **305**, 567–580 (2001).
[10] J.P. Overington, B. Al-Lazikani and Al.L. Hopkins, “How many drug targets are there?”, Nat Rev Drug Discov **5**, 993-996 (2006).
[11] J.E. Morgan et al., “Structure changes upon deprotonation of the proton release group in the bacteriorhodopsin photocycle”, Biophys J **103**, 444–452 (2012).
[12] R. F. Kubin and A. N. Fletcher, “Fluorescence quantum yields of some rhodamine dyes”, J. Luminescence **27,** 455–462 (1982).